

Microstructure changes in superplastically deformed ultrafine-grained Al-3Mg-0.2Sc alloy

P. Kral^{1,2}, J. Dvorak^{1,2}, M. Kvapilova^{1,2}, Z. Horita³, V. Sklenicka^{1,2†}

†vsklen@ipm.cz

¹Institute of Physics of Materials, Academy of Sciences of the Czech Republic, Žižkova 22, 616 62 Brno, Czech Republic

²CEITEC-IPM, Institute of Physics of Materials, Academy of Sciences of the Czech Republic, Žižkova 22, Brno, Czech Republic

³Department of Materials Science and Engineering, Faculty of Engineering, Kyushu University, Fukuoka 812-8581, Japan

Experiments were conducted on an ultrafine-grained Al-3wt.%Mg-0.2wt.%Sc alloy to characterize the microstructure changes occurring during large tensile deformation at elevated temperature within a transition between superplasticity and creep. The coarse-grained material was subjected to equal-channel angular pressing at room temperature using a die which had a 90° angle between the channels. The billets were rotated by 90° in the same sense between each pass in the processing route Bc. The billets were subsequently pressed by 2 and 8 passes. Microstructure was investigated by scanning electron microscope equipped with an electron back scatter diffraction unit. Microstructure analysis showed that the movement of dislocations and the growth of grains were restricted by Al₃Sc coherent precipitates formed during stabilizing annealing at 623 K for 1h. It was found that deformation behaviour of investigated Al alloy was influenced by inhomogeneity of microstructure and deformation-induced coarsening of grains. The fracture behaviour was affected by cavity formation due to high local concentration of plastic deformation at the triple points and inefficient accommodation processes of grain boundary sliding. The results showed that total tensile deformation is a consequence of a various mechanisms occurring at different stages of tensile deformation. The superplastic tensile deformation was predominantly realized by grain boundary sliding and formation of mesoscopic shear bands. The role played by grain boundary sliding is discussed.

Keywords: ultrafine-grained microstructure, aluminium alloy, equal-channel angular pressing, electron back scatter diffraction

Изменения микроструктуры в сверхпластически деформированном ультрамелкозернистом сплаве Al-3Mg-0.2Sc

Проведены эксперименты на ультрамелкозернистом сплаве Al-3 вес.% Mg-0.2 вес.% Sc с целью выяснения изменений микроструктуры, происходящих при большой деформации растяжением при высокой температуре в области перехода между сверхпластичностью и ползучестью. Крупнозернистый материал был подвергнут равноканальному угловому прессованию при комнатной температуре с использованием оснастки, имеющей угол 90° между каналами. В соответствии с маршрутом обработки B_c образцы между двумя последовательными переходами поворачивались на угол 90° в одном и том же направлении. Образцы были деформированы путем 2 и 8 проходов. Микроструктура была исследована с помощью сканирующего электронного микроскопа, оборудованного приставкой для дифракции обратно рассеянных электронов. Анализ микроструктуры показал, что движение дислокаций и рост зерен сдерживаются когерентными включениями Al₃Sc, образующимися при стабилизирующем отжиге при 623 K в течение 1 ч. Показано, что на деформационное поведение исследованного сплава Al влияет неоднородность микроструктуры и деформационно-индуцированное укрупнение зерен. На характер разрушения влияет образование пор из-за высокой локальной концентрации пластической деформации около тройных стыков и неэффективная аккомодация процессов зернограницного проскальзывания. Результаты показали, что полная деформация растяжением является следствием различных механизмов, имеющих место на различных стадиях деформации растяжением. Сверхпластическая деформация растяжением преимущественно реализуется путем зернограницного проскальзывания и образования мезоскопических полос сдвига. Обсуждена роль, которую играет зернограницное проскальзывание.

Ключевые слова: ультрамелкозернистая микроструктура, алюминиевый сплав, равноканальное угловое прессование, дифракция обратно рассеянных электронов

1. Introduction

Methods of severe plastic deformation [1] enable to reduce grain size to the submicrometer or even nanometer level. The effective technique is equal-channel angular pressing (ECAP) [1]. The materials with ultrafine-grained (UFG) structure may have different mechanical properties in comparison with coarse-grained materials. It can be expected that the reduction of the grain size to UFG region leads to a change of the creep deformation mechanism (s) in comparison with coarse-grained materials. Recent works [2–7] demonstrated that it is possible to achieve high ductility in Al alloys processed by ECAP. Experiments on the Al – 3% Mg – 0.2%Sc alloy showed that processing by ECAP reduced the grain size to about $\sim 0.2 \mu\text{m}$ and subsequent tensile testing gave elongations up to $>2000\%$ when testing with initial strain rates from 10^{-3} to 10^{-1} s^{-1} [2,3]. It was shown that the ultrafine grain sizes introduced by ECAP are reasonably stable at the high temperatures required for superplastic flow. Thus, it is possible to achieve high tensile ductility in ECAP aluminum alloys tested at very rapid strain rates [3–7] including the rates associated with high strain rate superplasticity which are defined formally as $\geq 10^{-2} \text{ s}^{-1}$ [8].

Superplasticity is a close phenomenon of thermal creep. Since superplastic deformation occurs at higher strain rates and higher stresses while creep occurs under relatively low applied stress for a longer exposure. One of the dominant common microstructural features in superplasticity and creep is the role played by grain boundary sliding (GBS). Therefore, it seems acceptable to associate superplastic and creep behaviour of UFG materials with more intensive grain boundary sliding due to smaller grain size [9,10], but there are probable further reasons strongly influencing the creep deformation mechanisms. It was found [11] that creep behaviour is influenced by formation of mesoscopic shear bands (MSBs). The long MSBs exceeding considerably the average grain size were observed in creep of UFG Al, Cu, Al-0.2Sc and Cu-0.2Zr alloys [11–13]. The formation of MSBs can significantly influence fracture processes and creep behaviour of ECAP materials [13]. Further creep fracture of pure Cu is influenced by considerable cavitation resulting from inefficient accommodation processes of GBS [14]. The creep behaviour of UFG materials may be influenced by synergetic effect of additional creep mechanisms like GBS, cavitation or more intensive diffusion processes. The influence of synergetic effect of additional creep mechanisms on creep behaviour of UFG materials may be supported by the value of stress exponent n often involving intragranular dislocation process and concurrently an observation of GBS or cavitation [15,16].

The grain boundary sliding is considered to be main deformation mechanism responsible for superplastic behaviour. The GBS is associated with grain rotation and from this reason it leads to the texture reduction. However, many works [17] based on texture analysis showed, that crystallographic slip forming certain texture may be also important in superplastic deformation. The aim of this work is to describe the microstructural changes occurring in the UFG Al-3Mg-0.2Sc alloy during tensile deformation at elevated temperature within the range corresponding to a transition between creep and superplastic behaviour of the alloy.

2. Material and methods

The ternary Al-Mg-Sc alloy was fabricated at the Department of Materials Science and Engineering, Faculty of Engineering, Kyushu University, Fukuoka, Japan.

The alloy was prepared by arc melting, in an argon atmosphere, Al of 99.99% purity and Sc of 99.999% purity to form initially an Al-3% Sc alloy, and this alloy was then remelted with additional Al and 3% Mg of 99.9% purity to give an Al-3% Mg-0.2% Sc alloy. The alloy was cast into a steel mold to form an ingot with dimensions of $17 \times 55 \times 120 \text{ mm}^3$, the ingot was homogenized in air at 753 K for 24 h. The ingot was cut into bars with dimensions of $15 \times 15 \times 120 \text{ mm}^3$ and these bars were swaged into rods having diameters of 10 mm. The rods were cut into cylindrical billets for with lengths of $\sim 60 \text{ mm}$ for ECA pressing. The billets were subjected to a solution treatment at temperature of 883 K for 1 h. The measured initial grain size after this solution treatment was $\sim 200 \mu\text{m}$.

The billets were processed by ECAP at room temperature using a die that had an internal angle of 90° between the two parts of the channel and an outer arc of curvature of $\sim 45^\circ$, where these two parts intersect. It can be shown from first principles that these angles lead to an imposed strain of ~ 1 in each passage of the sample [1]. The pressing speed was 19 mm/s. The billets were subsequently pressed by route B_c by 2 and 8 ECAP passes to give the mean grain size $\sim 0.2 \mu\text{m}$. In order to exclude a thermal instability of the grain structure during tensile testing the specimen was heated at 623 K for 1 h prior to test. The tensile sample, having the gauge length of 12 mm and cross-sectional areas of $3 \times 1.5 \text{ mm}^2$, was machined from billets parallel to the section XZ [11]. The tensile testing was conducted in an environment of purified argon with the testing temperature maintained to within $\pm 0.5 \text{ K}$ of the desired value. The microstructure was examined by transmission electron microscope (TEM) and scanning electron microscope (SEM) equipped by electron back scatter diffraction (EBSD).

3. Experimental results

Tensile testing

Figure 1 shows the results for two ECAP pressed specimens tensile tested at the same initial strain rate 10^{-4} s^{-1} which attained different true strain prior to fracture. The higher elongation $\sim 500\%$ was attained in the specimen processed by 8 ECAP passes indicating the occurrence of superplasticity. By contrast, relatively low elongation $\sim 150\%$ was obtained in the specimen processed by 2 ECAP passes. The following microstructural analyses were conducted to provide an explanation for such different behaviour.

Microstructure of the Al-3Mg-0.2Sc alloy

Figure 2a exhibits TEM micrograph of an annealed specimen, which demonstrates the presence of coherent Al₃Sc precipitates within the alloy matrix. Al₃Sc precipitates are indicated by a coherency strain contrast that appears in

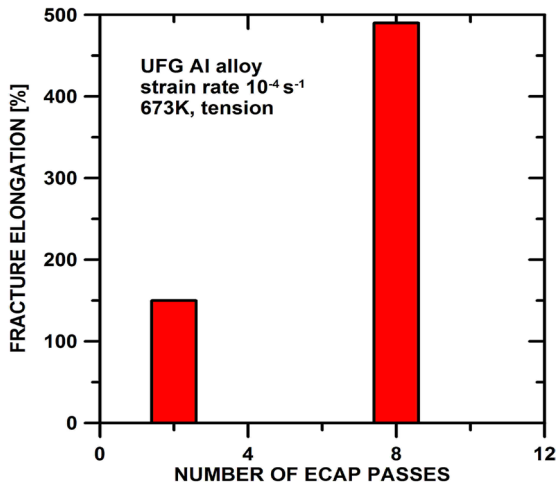
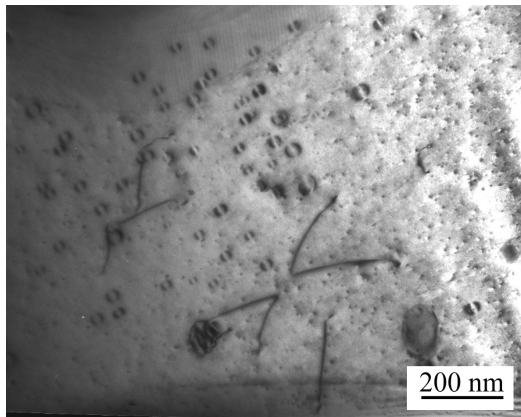
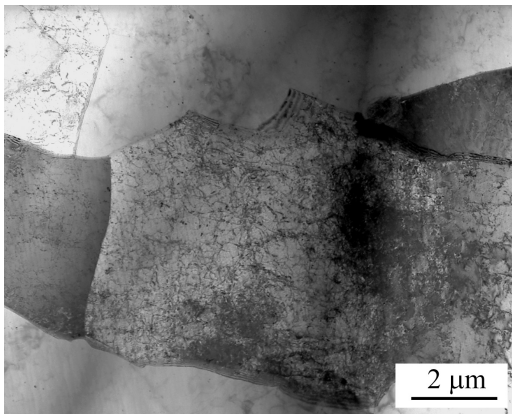


Fig. 1. The dependence of fracture elongation vs. number of ECAP passes.

this micrograph. Fig. 2b shows dislocation microstructure observed after creep exposure of UFG alloy. The dislocation pairs present in the alloy containing the smallest precipitate radii are very frequent. For larger precipitates the dislocations are pinned efficiently by Al_3Sc precipitates as climbing becomes slower. The microstructure of UFG Al alloy was investigated at different sites of superplastically deformed tensile specimen.

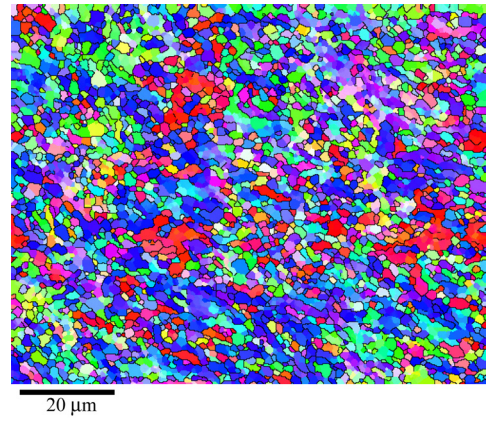


a

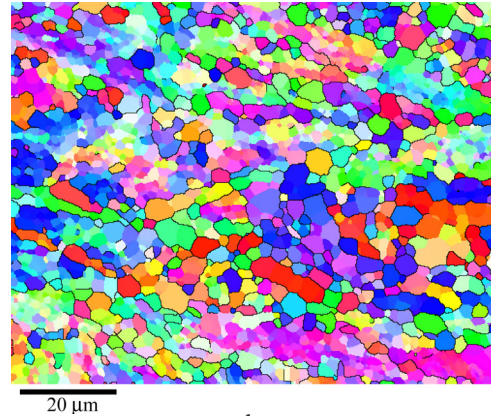


b

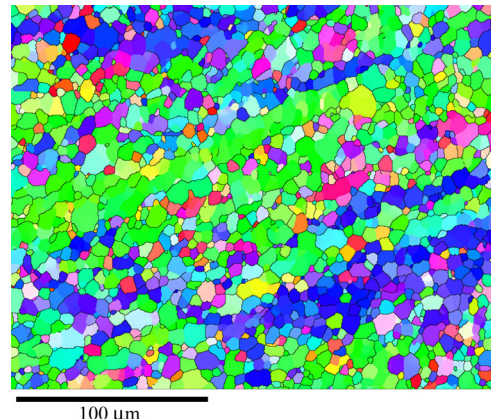
Fig. 2. Microstructure of the UFG Al-Mg-Sc alloy processed by 8 ECAP passes: (a) coherent Al_3Sc precipitates, (b) dislocation microstructure after creep.



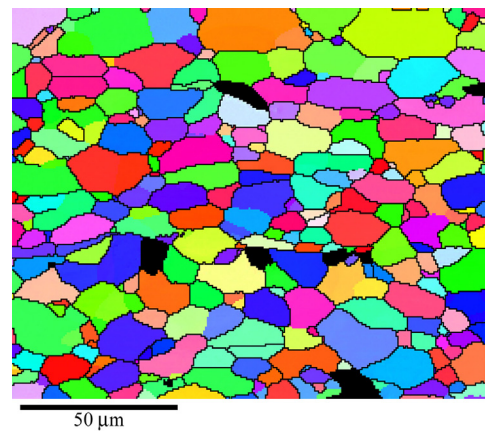
a



b



c



d

Fig. 3. Microstructure of the UFG Al-Mg-Sc alloy processed by 8 ECAP passes: (a) after stabilizing annealing at 623 K for 1 h (prior to tensile testing), (b) in the head of tensile specimen, (c) in the gauge length and (d) in the fracture area.

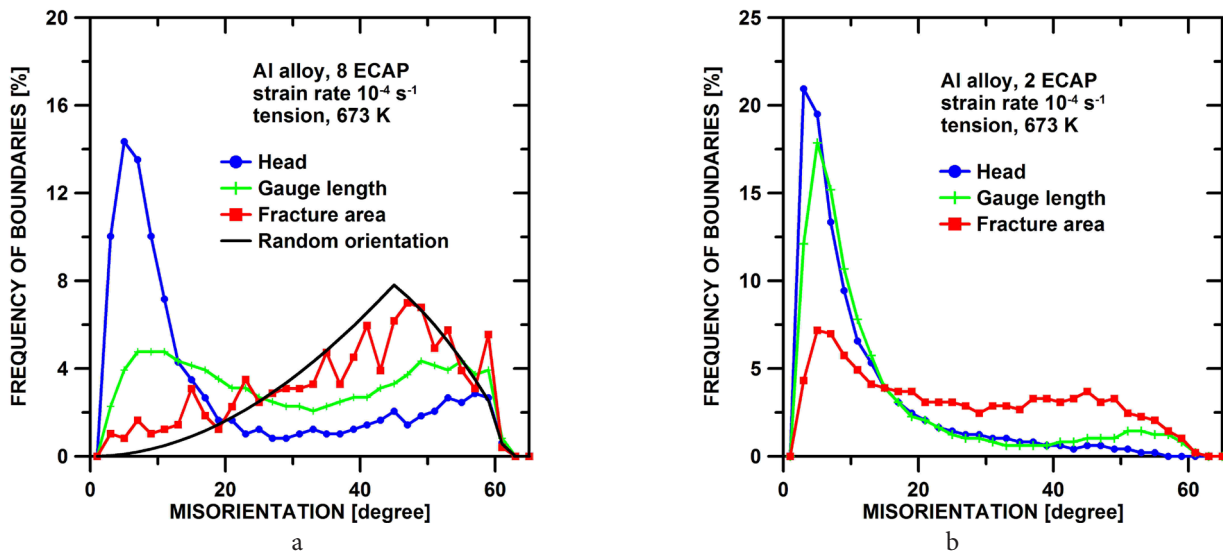


Fig. 4. The distribution of misorientation angle in the microstructure processed by: (a) 8 and (b) 2 ECAP passes and subsequently tested at 673 K.

The microstructure changes occurring during tensile testing at 673 K are shown in Fig. 3 for example after ECAP for 8 passes. It can be seen that stabilizing annealing at 623 K for 1 h before tensile testing caused grain growth up to $\sim 0.9 \mu\text{m}$ (Fig. 3a). The EBSD analyses showed that misorientation measured in the head of specimen (Fig. 3b) tested at 673 K contained (sub)grains with mean size about $1.5 \mu\text{m}$. In the head was measured about 41% of HAGBs (Fig. 4a).

Microstructure observed in the gauge length of the deformed specimen (Fig. 3c) had mean (sub)grain size $\sim 4.2 \mu\text{m}$. The microstructure had a bimodal character and contained large elongated areas with similar orientation oriented close to 45° to the tensile direction. The detailed inspection of EBSD data revealed that in the microstructure contained about $\sim 75\%$ of HAGBs. The misorientation distribution of boundaries had a bimodal character (Fig. 4a). The first group of boundaries is formed by low angle grain boundaries (LAGBs) and HAGBs situated mostly inside of the large elongated grains. The second group of boundaries is formed by HAGBs of large elongated and fine grains. The superplastic deformation led to the significant grain

growth (Fig. 3d). The grain size measured in the fracture area was $\sim 7.5 \mu\text{m}$. The microstructure contained $\sim 93\%$ of HAGBs (Fig. 4a) and the misorientation distribution showed that misorientation angles of boundaries are close to the distribution of misorientation angles for a randomly textured material [18].

Microstructure of Al alloy processed by 2 ECAP passes after tensile exposure had the mean grain size $\sim 6.8 \mu\text{m}$. However microstructure had a bimodal character and contained long shear bands considerably exceeding average grain size (Fig. 5a). The shear bands were oriented close to the shear plane of the last ECAP pass.

The microstructure in the head contained $\sim 25\%$ of HAGBs (Fig. 4b) and their frequency increases with additional tensile deformation up to $\sim 65\%$ of HAGBs in the fracture area.

Damage and fracture behaviour

The detailed microstructural analysis was performed on superplastically deformed specimen processed by 8 ECAP passes.

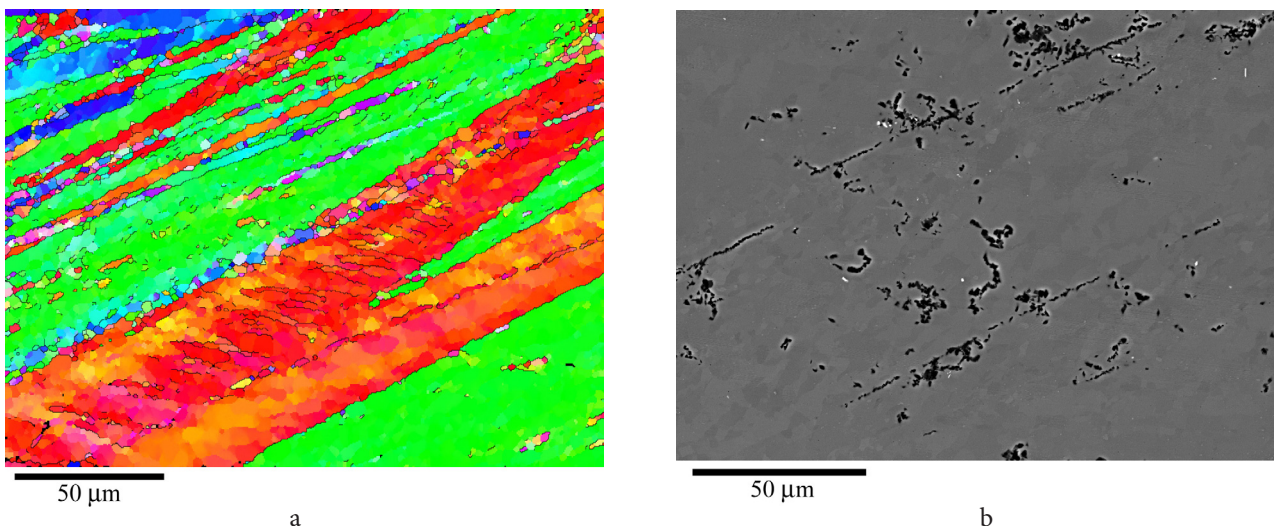


Fig. 5. Microstructure of Al alloy processed by 2 ECAP passes (a) mesoscopic shear bands, (b) cavitation on fracture surface.

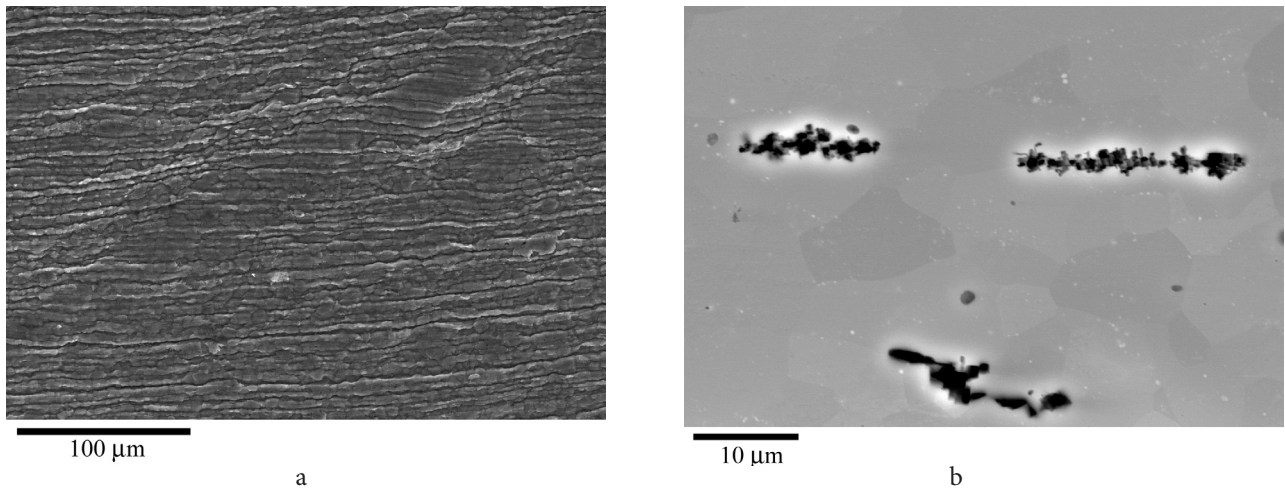


Fig. 6. The fracture surface of the UFG Al-Mg-Sc alloy (8 ECAP passes) (a) gauge length, (b) near fracture area.

The investigation revealed the formation of mesoscopic shear bands on the specimen surface along the gauge length and cavitation in the fracture area (Fig. 6a). The cavities nucleate, coalesce and propagate along grain boundaries (Fig. 6b). In the fracture area and also in the gauge length were observed cavities aligned parallel to the stress axis (Fig. 6b). Fig. 7a,b shows typical cavitation fracture of UFG Al alloy. The final fracture is associated with cavity interlinkage without the development of any significant necking.

The ECAP specimen processed by 2 passes showed an intrinsic plastic fracture with clear evidence for necking. There was a lack of cavitation damage in comparison with previous specimen exhibited higher elongation to fracture. The investigation of damage behaviour found that cavities preferentially propagate close the direction of shear bands orientation (Fig. 5b).

4. Discussion

The microstructure investigation revealed that the precipitate strengthened UFG Al-Mg-Sc alloy is unstable during static

annealing at 623 and 673 K. It is consistent with previous results which observed that the grain growth occurred at temperature higher than 573 K [2]. Nevertheless, the mean (sub)grain size of this alloy was still near UFG region.

Investigation of microstructure showed the formation of large elongated areas (strips) significantly exceeding average (sub)grains size in the gauge length. The presence of these areas in the microstructure can be associated with the formation of MSBs on specimen surface. The formation of MSBs has been observed during creep of Al-Sc, Cu-Zr alloys and it was suggested that the formation of MSBs significantly influence the elongation of UFG materials. It should be noted that Kaibyshev et al. [19] also observed that superplastic flow is localized within a set of deformation bands. They suggested a physical model of superplastic deformation based on cooperative boundary sliding of grain clusters [20].

It is generally accepted that the co-existence of larger grains in the bimodal structure can improve deformation behavior of UFG materials by relaxation of stress concentration, created by grain boundary sliding (GBS), inside of larger grains [21]. In this regard bimodal microstructure allows the simultaneous occurrence of dislocation slip and GBS. The

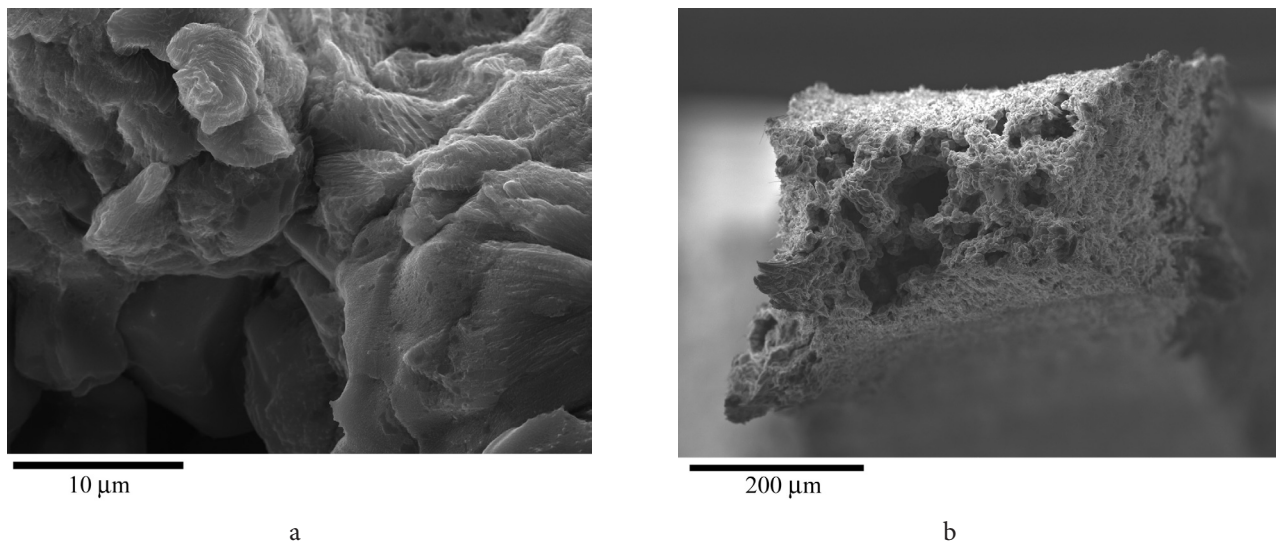


Fig. 7. Intergranular fracture of the UFG Al-Mg-Sc alloy (8 ECAP passes) after superplastic deformation

misorientation distribution and texture formation support this suggestion. Two peak misorientation distribution of boundaries can be explained by formation of certain preferential orientation due to crystallographic slip (first group of boundaries) and random grain orientation with maximum about 45° due to GBS (second group of boundaries).

The large deformation in the fracture area led to the significant grain growth and formation of random grain orientation. The misorientation distribution following the Mackenzie distribution for randomly oriented cubes [18] can be connected with GBS involving grain rotations. The presence of GBS during tensile deformation is supported by observed formation of cavities at triple points. The occurrence of cavities is the result of high local concentration of plastic deformation at the triple points and inefficient accommodation processes of GBS.

In the microstructure, there were elongated cavities parallel with tensile axis. The formation of these cavities could be connected with plasticity-controlled growth during superplastic flow in UFG materials [22—24]. It has been reported that superplastic alloys exhibit a transition from superplastic diffusion growth of cavities to plasticity-controlled growth with increasing cavity radius [24].

Kawasaki et al. [24] studied cavitation in a superplastic spray-cast Al-7034 alloy processed by ECAP and they concluded that superplastic diffusion growth is an important mechanism for cavity growth in ultrafine-grained materials processed by ECAP. They anticipated that superplastic diffusion growth is more significant growth mechanism when strain rate is reduced because the value of critical radius is then increased.

However, in the present work it was observed that grains grow significantly during tensile deformation. It can be suggested that in this case the superplastic diffusion growth is less important due to larger grain size. In superplastic materials are grains very small and cavities may insert a number of different boundaries so that vacancies enter cavity along many different boundary paths.

On the basis of present results it can be suggested that superplastic diffusion was limited in present UFG alloy due to deformation — induced growth of grains. Nevertheless some cavities reached critical radius and were able to grow by plasticity-controlled growth. The deformation-induced coarsening of grains led to the suppression of superplastic diffusion growth and plasticity-controlled growth was enhanced.

The high relative fractions of LAGBs population in the specimen processed by 2 ECAP passes (Fig. 4) may reflect some restriction in the extent of GBS and lower ductility of the specimen. However, there are probable further reasons strongly influencing an intragranular deformation mechanism. Subgrain formation requires both dislocation cross-slip and climb to enable rapid rearrangement of dislocation [25—27]. A model which describes the high temperature deformation response of the resulting dislocation substructure was developed by Blum et al. [28,29] based on earlier model of Mughrabi [30,31]. This model supposes that each grain includes the cells with thin walls containing dense arrays of dislocations and the cell interiors containing a low density of dislocations. The dislocations in the cell walls produce a large resistance to the motion of dislocations through the walls

[30,31]. As a result, some dislocations in the cell interiors are held up at the interface between cell walls and cell interiors. At the cell interiors, the dislocations are arranged randomly as a three dimensional network structure, which has been confirmed by TEM observation [32].

Finally, the same Al-3Mg-0.2Sc alloy processed by ECAP was creep tested at 473 K using strain rate from 10^{-7} to 10^{-5} s^{-1} [32—34]. The ultrafine-grained Al-3Mg-0.2Sc alloy exhibited faster creep, by about two to three orders of magnitude, than the unpressed alloy under the same loading conditions. This detrimental effect of ECAP was explained by increasing contribution of GBS to the total creep strain.

Conclusions

The microstructure analyses found that superplastic deformation of the alloy under investigation is influenced by inhomogeneity of microstructure after ECAP and deformation-induced coarsening of grains. The superplastic tensile deformation is predominantly realized by grain boundary sliding and formation of mesoscopic shear bands.

Acknowledgements. Financial support for this work was provided by CEITEC - Central European Institute of Technology with research infrastructure supported by the project CZ.1.05/1.1.00/02.0068 financed from European Regional Development Fund.

References

1. R.Z. Valiev, R.K. Islamgaliev, I.V. Alexandrov. *Prog. Mater. Sci.* **45**, 103 (2006).
2. S. Komura, M. Furukawa, Z. Horita, M. Nemoto, T.G. Langdon. *Mater. Sci. Eng. A* **297**, 111 (2001).
3. C.G. Sakai, Z. Horita, T.G. Langdon. *Mater. Sci. Eng.* **393**, 344 (2005).
4. S. Lee, A. Utsunomiya, H. Akamatsu, K. Neishi, M. Furukawa, Z. Horita, T.G. Langdon. *Acta Mater.* **50**, 553 (2002).
5. C. Xu, M. Furukawa, Z. Horita and T.G. Langdon. *Acta Mater.* **51**, 6139 (2003).
6. C. Xu, T.G. Langdon. *Mater. Sci. Eng. A* **410—411**, 398 (2005).
7. M. Kawasaki, C. Xu, T.G. Langdon. *Acta Mater.* (2005)
8. Z. Horita, M. Furukawa, M. Nemoto, A.J. Barnes, T.G. Langdon. *Acta Mater.* **48**, 3633 (2000).
9. M. Kawasaki, T.G. Langdon. *J. Mater. Sci.* **48**, 4730 (2013).
10. M. Kawasaki, R.B. Figueiredo, T.G. Langdon. *Letters on Mater.* **4**, 78 (2014).
11. P. Kral, J. Dvorak, V. Sklenicka. *Mater. Sci. Forum.* **584—586**, 846 (2008).
12. P. Kral, J. Dvorak, P. Seda, A. Jäger, V. Sklenicka. *Rev. Adv. Mater. Sci.* **31**, 14 (2012).
13. V. Sklenicka, P. Kral, J. Dvorak, M. Kvapilova, M. Kawasaki, T.G. Langdon. *Mater. Sci. Eng.* **667—669**, 897 (2011).
14. V.I. Betekhtin, A.G. Kadomtsev, P. Kral, J. Dvorak, M. Svoboda, I. Saxl, V. Sklenicka. *Mater. Sci. Forum*

- 567—568, 93 (2008).
15. V. Sklenicka, J. Dvorak, M. Svoboda. *Mater. Sci. Eng. A* **387—389**, 696 (2004).
 16. P. Kral, J. Dvorak, S. Zherebtsov, G. Salishchev, M. Kvapilova, V. Sklenicka. *J. Mater. Sci.* **48**, 4789 (2013).
 17. M.E. Kassner. *Fundamentals of Creep in Metals and Alloys*. Amsterdam, Elsevier (2009).
 18. J.K. Mackenzie. *Biometrika* **45**, 229 (1958).
 19. O. A. Kaibysev, V. V. Astanin, S. N. Faizova. *Trans. Mater. Res. Soc. Japan* **16B**, 1473 (1994).
 20. O. A. Kaibyshev, A. I. Pshenichniuk, V. V. Astanin. *Acta Mater.* **46**, 4911 (1998).
 21. Y.M. Wang, M. V. Chen, F.H. Zhou, E. Ma. *Nature* **419**, 912 (2002).
 22. M. Kawasaki, Y. Huang, Che. Xu, M. Furukawa, Z. Horita, T.G. Langdon. *Mater. Sci. Eng. A* **410—411**, 402 (2005).
 23. R. Figueiredo, T.G. Langdon. *Metal. Mater. Trans. A* **45A**, 3197 (2014).
 24. M. Kawasaki, Ch. Xu, T.G. Langdon. *Acta Mater.* **53**, 5353 (2005).
 25. O. D. Sherby. *Acta Metall.* **10**, 135 (1962).
 26. S.I. Hong, C. Laird. *Acta Metall. Mater.* **38**, 1581 (1990).
 27. B. Chen, P.E. J. Flewitt, A. C. F. Cocks, D.J. Smith. *Inter. Mater. Rev.* **60**, 1 (2015).
 28. H. Hider, W. Blum. *Mater. Sci. Eng. A* **164**, 290 (1993).
 29. R. Sedlacek, W. Blum. *Comp. Mater. Sci.* **25**, 200 (2002).
 30. H. Mughrabi. *Acta Metall.* **31**, 1367 (1983).
 31. H. Mughrabi. *Mater. Sci. Eng. A*. **85**, 15 (1987).
 32. V. Sklenicka, J. Dvorak, M. Svoboda, P. Kral, M. Kvapilova, in: Z. Ahmad (Ed.), *Aluminium Alloys — New Trends in Fabrication and Applications*. InTech (2012), p.3. ISBN 978-953-51-0861-0.
 33. V. Sklenicka, J. Dvorak, M. Svoboda, P. Kral, M. Kvapilova, Z. Horita, in: Y.T. Zhu et al. (Eds.), *Ultrafine Grained Materials IV*, TMS (2006), p.459.
 34. M. Kawasaki, V. Sklenicka, T.G. Langdon. *Kovove Mat.* **49**, 75 (2011).